Journal of Magnetism and Magnetic Materials 324 (2012) 11–14

Contents lists available at ScienceDirect

Journal of Magnetism and Magnetic Materials

journal homepage: www.elsevier.com/locate/jmmm

Magnetic Barkhausen emission in lightly deformed AISI 1070 steel

J. Capó Sánchez [a,*], M.F. de Campos [b], L.R. Padovese [c]

[a] Departamento de Física, Facultad de Ciencias Naturales, Universidad de Oriente, Av. Patrıcio Lumumba s/n, 90500 Santiago de Cuba, Cuba
[b] EEIMVR—Universidade Federal Fluminense, Av. dos Trabalhadores 420, Vila Santa Cecilia, 27255-125 Volta Redonda, RJ, Brazil
[c] Departamento de Engenharia Mecânica, Escola Politécnica, Universidade de São Paulo, Av. Prof. Mello Moraes, 2231, 05508-900 São Paulo, Brazil

ARTICLE INFO

Article history:
Received 9 April 2011
Received in revised form
11 July 2011
Available online 28 July 2011

Keywords:
Magnetic Barkhausen emission
Strain
Residual stress
X-ray diffraction

ABSTRACT

The Magnetic Barkhausen Noise (MBN) technique can evaluate both micro- and macro-residual stresses, and provides indication about the relevance of contribution of these different stress components. MBN measurements were performed in AISI 1070 steel sheet samples, where different strains were applied. The Barkhausen emission is also analyzed when two different sheets, deformed and non-deformed, are evaluated together. This study is useful to understand the effect of a deformed region near the surface on MBN. The low permeability of the deformed region affects MBN, and if the deformed region is below the surface the magnetic Barkhausen signal increases.

1. Introduction

Most of the structural steels are obtained through mechanical processes that cause elastic or plastic deformations, such as rolling, drawing and extrusion. These processes can also generate noticeable magnetic anisotropy in the material [1,2] because the magnetic behavior of the steel strongly depends on its stress–strain state [3,4]. Small plastic deformation leads to the debility of the magnetic Barkhausen emission (MBN) [5,6] in AISI 1070 steel. Therefore, the combined effects of plastic slip and residual stresses produce modifications at a microstructural level.

There are two main types of elastic stresses: (i) microstresses around dislocations (order of Angstroms) and (ii) elastic macrostresses along the length of the sample [7,8]. These two types of elastic stresses have different effects on MBN and hysteresis. Besides, for heavily deformed steels (above 8% of deformation), tangles dislocations are formed [9], originating pinning of domain walls. In this study uniaxial stress was applied in the rolling direction of the samples, producing light deformation up to 3%. How to interpret the effects of macro- and microstress by means of MBN measurements and X-ray diffraction (XRD) analysis will be discussed.

2. Experimental setup

A cold rolled and annealed AISI 1070 steel sheet was selected for the investigation. Its chemical composition is given in Table 1. For all experimental measurements, the used samples (25 mm × 250 mm × 0.97 mm) were made of this commercial AISI 1070 steel. The samples were cut along the rolling direction of the annealed cold rolling sheet.

These samples were subjected to a strain rate of approximately 0.5 mm/min in a uniaxial stress–strain testing machine.

The present work studied samples "as received", that is, not subjected to this deformation process, and samples with additional relative deformations of 0.4%, 0.8%, 1.0% and 3.0%, produced by the mentioned stress–strain machine.

Measurement of MBN signals was performed by using a portable equipment developed at the laboratory named "BarkTech" (see Fig. 1). The data shown in Fig. 2 were obtained using a sinusoidal magnetic wave of 10 Hz and a magnetic field of 1.2×10^4 A/m. The MBN signal was detected using a pickup coil. The MBN sensor output was amplified and band pass filtered (1–150 kHz). The magnetizing yoke, pickup coil and samples were placed in a grounded steel box to reduce environmental noise.

The pickup coil, which measured the normal component of the MBN signal, was constructed by winding wire around a small cylindrical plastic bobbin. Special attention was given to the cable parasite capacitance, in order to maintain this characteristic constant.

The integral in the time domain of the voltage square of all MBN events represents the parameter known as the MBN energy (MBN_{energy}). This magnitude is calculated for 10 MBN measurements at each point of the sample and then averaged for each. Using a bottom voltage level, the noise not belonging to the Barkhausen signal was eliminated from the MBN measurements.

XRD measurements for the stress characterization were performed in Shimadzu 6000 equipment, with Co K_α radiation, using a graphite secondary monochromator.

* Corresponding author. Fax: 53 22 63 2689.
E-mail addresses: jcapo@cnt.uo.edu.cu, jcapo@usp.br (J. Capó Sánchez).

0304-8853
doi:10.1016/j.jmmm.2011.07.014

3. Results and discussion

In Fig. 2(a) the MBN data for 3 types of sheet configurations are presented (see Fig. 2(b)): (i) Simple-only one sheet, (ii) down-deformed above the non-deformed ("Down") and (iii) up-deformed below the non-deformed ("Up"). Fig. 2(b) shows that for the configurations (i) and (ii) a very small deformation (0.4%) significantly changes the MBN energy, and then on increasing the strain the MBN almost does not decrease. However, for the configuration (iii) a totally different behavior is observed, and an increased strain increases the MBN signal. The explanation for the result of configuration (iii) is that the magnetic flux tends to flow in the non-deformed sample, when the permeability of the sample is reduced, with increasing deformation.

Plastic deformation reduces the permeability [10]. The results of Fig. 2 show that the magnetic flux deviates and passes through regions of higher permeability (for our samples, it is the non-deformed sheet). This result confirms that MBN evaluates a portion of the sample near the surface, because the MBN emissions for the Down and Simple conditions is very similar.

MBN evaluates stress in a region very near to the surface, but not at the same range of the XRD analysis. The depth evaluated with XRD for steels under the Co K_α radiation is up to 20 μm. As the sample thickness is 1 mm, the magnetic flux penetrates more than this length. In other words, MBN evaluates a wider range than XRD. A very interesting result is found for the configuration (iii) ("Up"). This result is a proof that the MBN comes from different depths, and may change according to the microstructure of the sample. It is interesting to note that XRD is also a non-destructive technique, and the XRD analysis could be combined with the MBN analysis.

In Fig. 3, the XRD peaks for the (1 1 0) plane are shown for each level of deformation. A shift of the XRD peaks is observed, but the FWHM remains almost constant (in fact, increases very slightly). FWHM provides an estimate of the micro-stresses by means of the Stibilitz equation [7,8,11]. The increase of dislocation density can also be estimated by FWHM (full width at half maximum of the XRD peak) [7].

As the FWHM almost does not change with increasing plastic deformation, this means that the dislocation density is only

Table 1
Steel samples composition (10^{-3} wt%).

AISI	C	Mn	P	S	Si	Al	Cu	Cr	Ni	Mo	Ti	Nb
1070	711	966	18	2.3	321	38	6.6	182	36.9	2.2	3.7	2

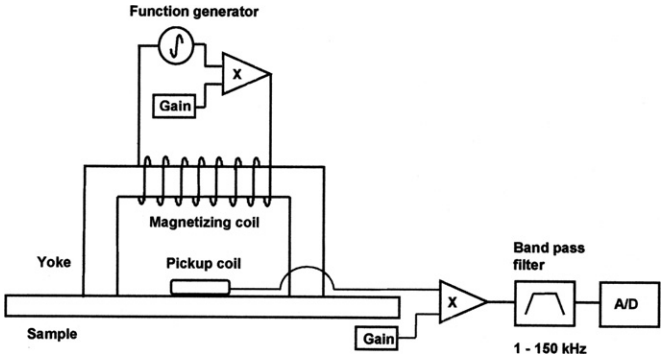

Fig. 1. Scheme of the employed setup.

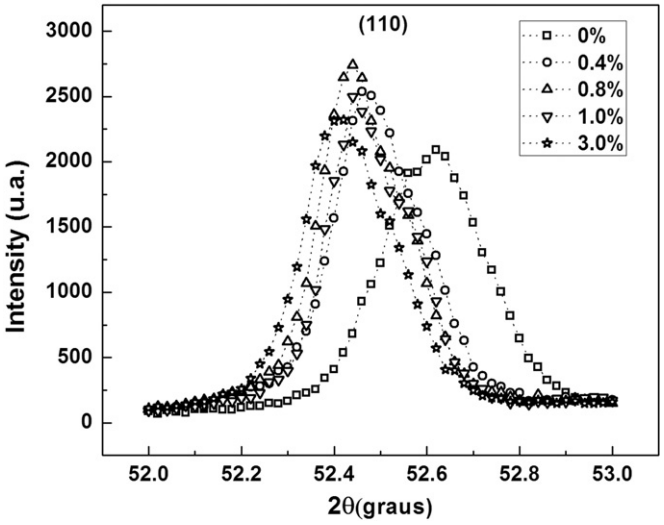

Fig. 3. XRD peaks for (1 1 0) direction in AISI 1070 steel samples.

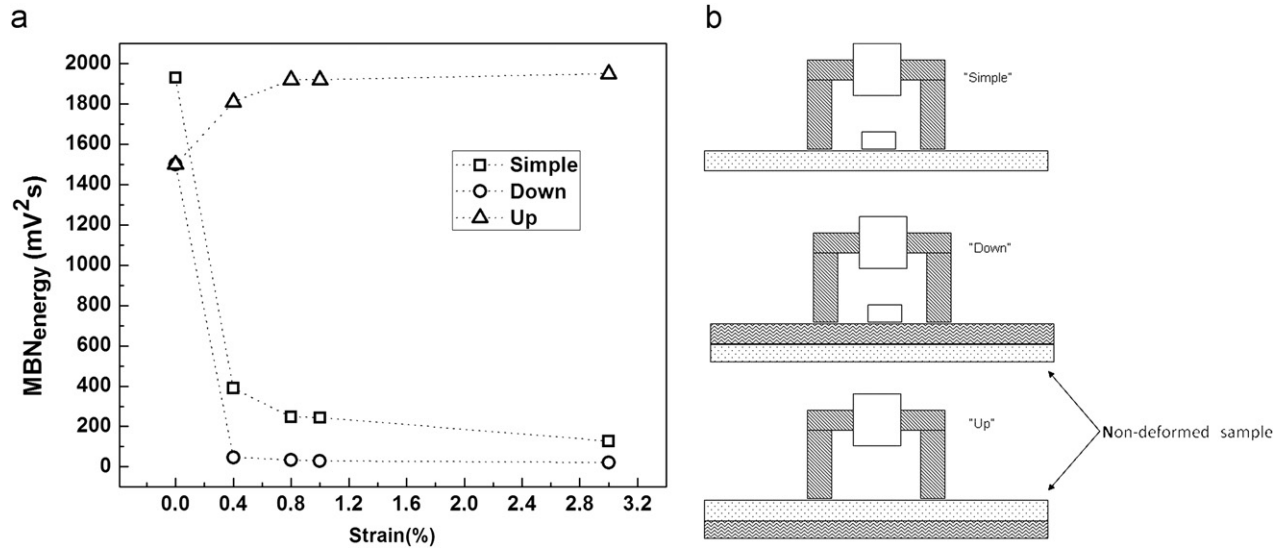

Fig. 2. MBN_{energy} dependence on strain (a) and sheet configurations (b).

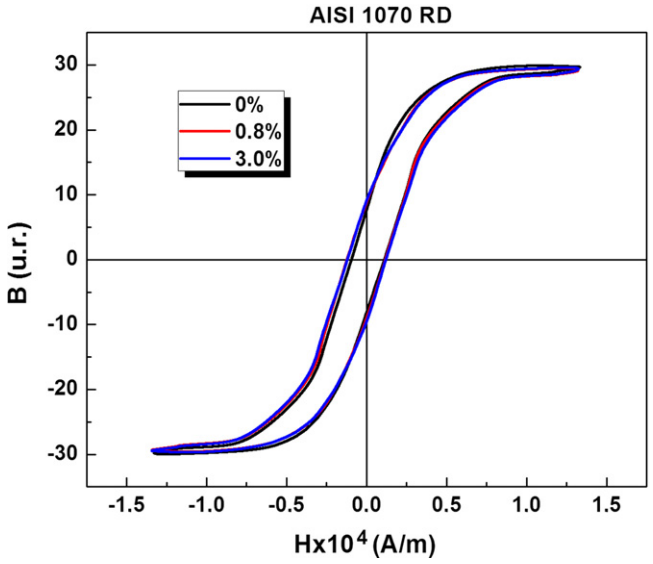

Fig. 4. Magnetic hysteresis curves for AISI 1070 steel samples. The field given in A/m is a relative field. *B* is given in relative units.

Table 2
Data processing of XRD.

Strain (%)	*khl*	2Θ (G)	*d* (Å)	*a* (Å)
0	110	52.61 ± 0.05	2.020 ± 0.001	2.856 ± 0.001
0.4	110	52.49 ± 0.05	2.024 ± 0.001	2.863 ± 0.001
0.8	110	52.46 ± 0.05	2.026 ± 0.001	2.864 ± 0.001
1.0	110	52.47 ± 0.05	2.025 ± 0.001	2.864 ± 0.001
3.0	110	52.43 ± 0.05	2.027 ± 0.001	2.866 ± 0.001

Table 3
Estimation of elastic stress in the measurement direction.

Stresses σ (GPa)			
0.4%	0.8%	1.0%	3.0%
0.42	0.48	0.40	0.60

slightly increased. However the shifts of the peaks are clear indication of the presence of macrostresses [12].

Another indication can be obtained from the hysteresis curve (see Fig. 4). Plastic deformation [7] increases the coercitivity force and the area of hysteresis. As hysteresis is almost the same for samples 0%, 0.8% and 3%, this also indicates that deformation by means of slip (which generates dislocations) was not significant. Thus, XRD data and hysteresis are in agreement, indicating that in the studied samples the main variable is elastic deformation (macro-residual stresses).

Fig. 4 shows Hysteresis curves for the samples. These curves were obtained from the magnetic circuit comprising the U-shaped yoke and sample surface (see scheme of Fig. 1 for details of the magnetic circuit). Both H and B are given in relative units. The hypothetical H field is related to the applied current I according to the expression $H=nI/L$, where n is the number of turns in the excitation coil, I is the applied current and L is the length of the magnetic circuit. A hypothetical magnetic induction B could also be estimated using data from Fig. 4 with expression [13]

$$B=\frac{1}{nA}\int\left(\frac{d\phi}{dt}\right)dt\ [\mathrm{T}] \tag{1}$$

where n is the number of turns of the coil around the yoke (see Fig. 1); A is the transverse area of the yoke [m^2] and $d\phi/dt$ is the variation of magnetic flux, or the voltage measured in the third coil (see Fig. 1). It is important to mention that the analysis presented in Fig. 4 presupposes that the magnetic permeability of the samples is lower than the permeability of the material of the yoke.

In Table 2, the lattice parameters are shown. This is the average for several planes. As discussed above, XRD only evaluates regions near the surface of the samples and this depth is around 10–20 μm near the surface for the studied samples. Thus, these lattice parameters represent the deformation only for the area very near the surface. In Table 2 it is observed that there is an increase of lattice parameters with the applied deformation, suggesting also an increase of the macro residual stresses.

A rough estimation of elastic stress in the direction of the measurement can be done by means of the expression $\sigma=\varepsilon E/\nu$ with $\varepsilon=(d_o-d_i)/d_o$ as shown in Table 3. It is assumed that $E=170$ GPa and $\nu=0.3$ [14].

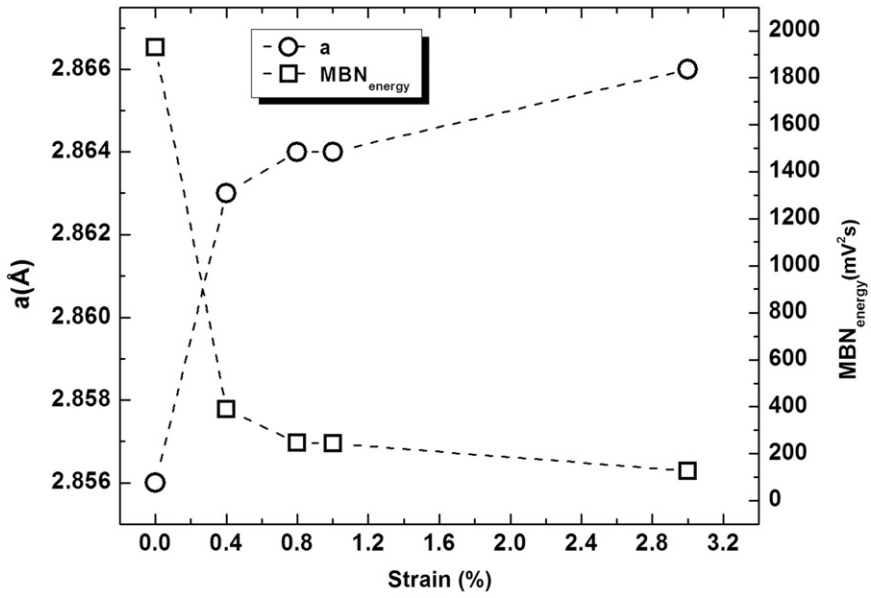

Fig. 5. Variations of MBN_{energy} and a parameter with strain for 1070 AISI steel.

In the graph of Fig. 5, a decrease of MBN_{energy} can be seen when deformation increases. The lattice parameters show a similar behavior; however they increase when ε deformation increases. The MBN results can also be analyzed by considering magnetostrictive effects [15]. Compressive stress results in reduction of MBN for magnetostrictive positive materials, whereas tensile stress increases MBN signal [16]. However, texture of the sample can also affect magnetostrictive properties [17] and the behavior found for the AISI 1070 samples is due to the specific texture of these sheets (texture means crystallographic orientation of the grains).

4. Conclusion

Both techniques XRD and MBN are non-destructive and can evaluate stress in a region near the surface of the samples. However, the depth obtained with MBN is larger.

For the AISI 1070 steel samples studied (where uniaxial stress was applied), the main effect on MBN seems to originate from macroelastic residual stress.

The results have shown that MBN is able to evaluate micro- and macro-residual stresses, and provides indication of the relevance of the contribution of these different stress components.

A very interesting result is found for the configuration (iii) or "up". In this case, the magnetic flux increases when the sheet below becomes more deformed. This can be attributed to the reduced permeability of the deformed samples, and as a consequence the magnetic circuit is closed in the proximity of the surface, thus increasing MBN. This result is a proof that MBN may originate from differences in depths, and varies according to the microstructure of the sample.

A "shielding" effect was observed:a sheet placed over the material that will be analyzed; changes all the results, but as the magnetic flux comes from surfaces the results essentially reflect the material that is close to the surface.

Acknowledgments

The authors would like to thank the financial support agencies CAPES (Project 052/08) and Fapesp (Project 05/1100–9).

References

[1] M. Delage, J.B. Ramiarinjaona, J.B. Desmoulins, J.F. Rialland, IEEE Trans. Magn. 33 (1997) 4038.
[2] F. Fiorillo, J. Magn. Magn. Mater. 304 (2006) 139.
[3] B.D. Cullity, Introduction to magnetic material, Addison-Wesley, London, 1972.
[4] D.G. Park, K.S. Ryu, S. Kobayashi, S. Takahashi, Y.M. Cheong, J. Appl. Phys. 107 (2010) 09A330.
[5] M. Alberteris Campos, J. Capó-Sánchez, J. Pérez Benítez, L.R. Padovese, NDT & E Int 41 (2008) 656.
[6] R. Hutanu, L. Clapham, R.B. Rogge, Appl. Phys. Lett. 86 (2005) 2503.
[7] M.F. Campos, M.J. Sablik, F.J.G. Landgraf, T.K. Hirsch, R. Machado, R. Magnabosco, C.J. Gutierrez, A. Bandyopadhyay, J. Magn. Magn. Mater. 320 (2008) e377.
[8] F. Burgahn, O. Vohringer, E. Macherauch, Phys. IV 01 (1991) 291.
[9] A.S. Keh, S. Weissman, Electron Microscopy and Strength of Crystals, Interscience, New York, 1963.
[10] F.J.G. Landgraf, M. Emura, J. Magn. Magn. Mater. 242 (2002) 152.
[11] G.R. Stibitz, Phy. Rev 49 (1936) 862.
[12] B.D. Cullity, Elements of X-Ray Diffraction, New York, 1978.
[13] M.F. de Campos, F.A. Franco, R. Santos, F.S. da Silva, S.B. Ribeiro, J.F.C. Lins, L.R. Padovese, J. Phys.: Conf. Ser. 303 (2011) 012030.
[14] W.F. Hosford, The Mechanics of Crystals and Textured Polycrystal, Oxford University Press, New York, 1993.
[15] F. Bohn, A. Gundel, F.J.G. Landgraf, A.M. Severino, R.L. Sommer, J. Magn. Magn. Mater. 317 (2007) 20.
[16] F. Coialori, Adv. Phy. 57 (2008) 287.
[17] T. Tomida, IEEE Trans. Magn. 38 (2002) 3186.